

\*

TTP96-24

MADPH-96-946

June 1996

## QCD Corrections to Jet Cross Sections in DIS

Erwin Mirkes<sup>a</sup> and Dieter Zeppenfeld<sup>b</sup><sup>a</sup>Institut für Theoretische Teilchenphysik, Universität Karlsruhe, D-76128 Karlsruhe, Germany<sup>b</sup>Department of Physics, University of Wisconsin, Madison, WI 53706, USA

Next-to-leading order corrections to jet cross sections in deep inelastic scattering at HERA are studied. The predicted jet rates allow for a precise determination of  $\alpha_s(\mu_R)$  at HERA over a wide range of  $\mu_R$ . We argue, that the “natural” renormalization and factorization scale is set by the average  $k_T^B$  of the jets in the Breit frame and suggest to divide the data in corresponding  $\langle k_T^B \rangle$  intervals. Some implications for the determination of the gluon density and the associated forward jet production in the low  $x$  regime at HERA are briefly discussed.

## 1. Introduction

Deep inelastic scattering (DIS) at HERA is a copious source of multi-jet events. Typical two-jet cross sections are in the 100 pb to few nb range and thus provide sufficiently high statistics for precision QCD tests [ 1]. Clearly, next-to-leading order (NLO) QCD corrections are mandatory on the theoretical side for such tests. Full NLO corrections for one and two-jet production cross sections and distributions are now available and implemented in the  $ep \rightarrow n$  jets event generator MEPJET, which allows to analyze arbitrary jet definition schemes and general cuts in terms of parton 4-momenta [ 2, 3]. A variety of topics can be studied with these tools.

1) The determination of  $\alpha_s(\mu_R)$  over a range of scales  $\mu_R$  from dijet production at HERA: The dijet cross section is proportional to  $\alpha_s(\mu_R)$  at leading order (LO), thus suggesting a direct measurement of the strong coupling constant. However, the LO calculation leaves the renormalization scale  $\mu_R$  undetermined. The NLO corrections substantially reduce the renormalization and factorization scale dependencies which are present in the LO calculations and thus reliable cross section predictions in terms of  $\alpha_s(m_Z)$  (for a given set of parton distributions) are made possible. Clearly, a careful study of the choice of

scale in the dijet cross section is needed in order to extract a reliable value for  $\alpha_s(M_Z)$ . We will present some arguments and studies of the scale dependence of the NLO dijet cross section which suggest that the average  $k_T^B$  of the jets in the Breit frame provides the “natural” scale for multi jet production in DIS. Here,  $(k_T^B(jet))^2$  is defined by  $2 E_j^2(1 - \cos \theta_{jP})$ , where the subscripts  $j$  and  $P$  denote the jet and proton, respectively (all quantities are defined in the Breit frame).

2) The measurement of the gluon density in the proton (via  $\gamma g \rightarrow q\bar{q}$ ): The gluon density can only be indirectly constrained by an analysis of the structure function  $F_2$  at HERA [ 4]. The boson gluon fusion subprocess dominates the two jet cross section at low  $x$  and allows for a more direct measurement of the gluon density in this regime. A first LO experimental analysis has been presented in [ 5]. NLO corrections reduce the factorization scale dependence in the LO calculation (due to the initial state collinear factorization, which introduces a mixture of the quark and gluon densities according to the DGLAP (Altarelli-Parisi) evolution) and thus reliable cross section predictions in terms of the scale dependent parton distributions are made possible. Some implications for the determination of the gluon density have been discussed in [ 3].

3) Associated forward jet production in the low  $x$  regime as a signal of BFKL dynamics: BFKL evolution [ 6] leads to a larger cross sec-

\*Invited talk presented by E. Mirkes. To appear in proceedings of “QCD and QED in Higher Orders” 1996 Zeuthen Workshop on Elementary Particle Theory, April 22-26, 1996.

tion for events with a measured forward jet (in the proton direction) with transverse momentum  $p_T^{lab}(j)$  close to  $Q$  than the DGLAP [ 7] evolution. Clearly, next-to-leading order QCD corrections for fixed order QCD, with Altarelli-Parisi (DGLAP) evolution, are mandatory on the theoretical side in order to establish a signal for BFKL evolution in the data. We discuss these corrections in section 3.

The importance of higher order corrections and recombination scheme dependencies of the two jet cross sections for four different jet algorithms (cone,  $k_T$  [ 8], JADE, W) was already discussed in [ 2, 3]. While the higher order corrections and recombination scheme dependencies in the cone and  $k_T$  schemes are small, very large corrections appear in the  $W$ -scheme. We conclude from these studies that the cone and  $k_T$  schemes appear better suited for precision QCD tests and will concentrate only on those schemes in the following.

The goal of a versatile NLO calculation is to allow for an easy implementation of an arbitrary jet algorithm and to impose any kinematical resolution and acceptance cuts on the final state particles. This is best achieved by performing all hard phase space integrals numerically, with a Monte Carlo integration technique. This approach also allows an investigation of the recombination scheme dependence of the NLO jet cross sections. For dijet production at HERA such a NLO Monte Carlo program is MEPJET[ 2]. The calculation is based on the phase space slicing method and on the technique of universal ‘‘crossing functions’’ [ 9, 10, 11]. More details are described in [ 2] and we do not repeat them here. This technique can also be extended to the case of massive quark production [ 12]. An alternative technique for the calculation of NLO corrections in jet physics is the ‘‘subtraction’’ method [ 13].

## 2. Choice of the Renormalization and Factorization Scale in Multijet Production

Jet production in DIS is a multi-scale problem and it is not a priori clear at which scale  $\alpha_s$  is probed. In the following we will discuss the choice of the renormalization and factorization scale for dijet production at HERA. As mentioned before,

the NLO corrections are expected to reduce the scale dependencies in the LO predictions provided the scale is of the order of the typical hardness of the partonic process.

The following studies are done for the cone algorithm (which is defined in the laboratory frame) and the distance  $\Delta R = \sqrt{(\Delta\eta)^2 + (\Delta\phi)^2}$  between two partons decides whether they should be recombined to a single jet. Here the variables are the pseudo-rapidity  $\eta$  and the azimuthal angle  $\phi$ . We recombine partons with  $\Delta R < 1$ . Furthermore, a cut on the jet transverse momenta of  $p_T(j) > 5$  GeV in the lab is imposed. We employ the two loop formula for the strong coupling constant with a value for  $\Lambda_{\overline{MS}}^{(4)}$  consistent with the value from the parton distribution functions. The value of  $\alpha_s$  is matched at the thresholds  $\mu_R = m_q$  and the number of flavors is fixed to  $n_f = 5$  throughout, *i.e.* gluons are allowed to split into five flavors of massless quarks. A running QED fine structure constant  $\alpha(Q^2)$  is used. In addition the following set of kinematical cuts is imposed on the initial virtual photon and on the final state electron and jets: We require  $40 \text{ GeV}^2 < Q^2 < 2500 \text{ GeV}^2$ ,  $0.04 < y < 1$ , an energy cut of  $E(e') > 10$  GeV on the scattered electron, and a cut on the pseudo-rapidity  $\eta = -\ln \tan(\theta/2)$  of the scattered lepton and jets of  $|\eta| < 3.5$ .

First studies of the scale dependence of the dijet cross section in the cone scheme are presented in [ 2]. We have considered scales related to the scalar sum of the parton transverse momenta in the Breit frame,  $\sum_i p_T^B(i)$ , and the virtuality  $Q^2$  of the incident photon. In the following we will also consider scales related to  $\sum_i k_T^B(i)$ . Here,  $(k_T^B(i))^2$  is defined by  $2 E_i^2(1 - \cos \theta_{iP})$ , where the subscripts  $i$  and  $P$  denote the final parton (or jet) and proton, respectively (all quantities are determined in the Breit frame). The Breit frame is characterized by the vanishing energy component of the momentum of the exchanged photon. Both the photon momentum

$$q = (0, 0, 0, -2xE), \quad -q^2 = Q^2 = 4x^2E^2 \quad (1)$$

and the proton momentum

$$P = E(1, 0, 0, 1) \quad (2)$$

are chosen along the  $z$ -direction.  $x$  is the standard Bjorken scaling variable. In the parton model, the incoming quark with momentum  $p = xE(1, 0, 0, 1)$  collides elastically with the virtual boson and is scattered in the opposite direction (the 'current hemisphere') with momentum  $p' = xE(1, 0, 0, -1)$ ; therefore,  $(k_T^B(p'))^2 = Q^2$  in the limit of the quark parton model, whereas  $p_T^B(p') = 0$ .

The kinematics for dijet production is more complex: the momentum fraction  $\eta$  of the incoming parton must be larger than  $x$  since  $m_{jj}^2 = Q^2(\eta/x - 1)$  and, in general, the jets have a non-vanishing transverse momentum with respect to the  $\gamma^*$ -proton direction. At LO, i.e. for massless jets, the relation between  $k_T^B(j)$  and  $p_T^B(j) = E_j \sin \theta_{jP}$  reads:

$$k_T^B(j) = p_T^B(j) \sqrt{\frac{2}{1 + \cos \theta_{jP}}} \quad (3)$$

Obviously,  $k_T^B(j) > p_T^B(j)$ , and one can also show that  $\sum_j k_T^B(j) > Q$ . Thus,  $\sum_j k_T^B(j)$  is approximately given by the harder of the two scales  $Q$  and  $\sum_j p_T^B(j)$  [14]. For large dijet invariant masses (i.e. for "true" two jet kinematics) one has  $\eta \gg x$ , the dijet system will be strongly boosted in the proton direction and  $k_T^B(j) \approx p_T^B(j) \gg Q/2$ , as long as very small scattering angles in the center of mass frame are avoided. For  $m_{jj} \approx Q$  or smaller, on the other hand,  $\sum_j k_T^B(j) \approx Q$  and, typically, both are considerably larger than  $\sum_j p_T^B(j) < m_{jj}$  (in particular for  $Q \gg m_{jj}$ , which corresponds to the parton model limit).

Thus  $\sum_j k_T^B(j)$  smoothly interpolates between the correct limiting scale choices, it approaches  $Q$  in the parton limit and it corresponds to the jet transverse momentum when the photon virtuality becomes negligible. It appears to be the "natural" scale for multi jet production in DIS.

In [2] we found that the scale dependence of the dijet cross section does not markedly improve in NLO for  $\mu^2 = \xi Q^2$ . This is also shown in Fig. 1 (dotted curves) where the dependence of the two-jet cross section on the scale factor  $\xi$  is shown. We used the parton distribution functions set MRS D' [15] and employed the two loop formula for the strong coupling constant both in the LO and

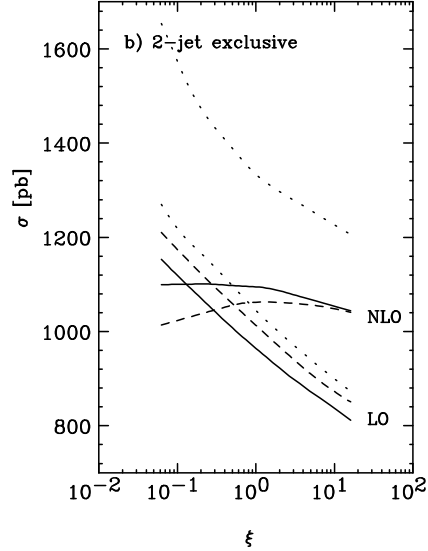


Figure 1. Dependence of the two-jet exclusive cross section in the cone scheme on the scale factor  $\xi$ . The dashed curves are for  $\mu_R^2 = \mu_F^2 = \xi (\sum_i p_T^B(i))^2$ . Choosing  $(\sum_i k_T^B(i))^2$  as the basic scale yields the solid curves. Choosing  $Q^2$  as the basic scale yields the dotted curves. Results are shown for the LO (lower curves) and NLO calculations.

NLO curves. For scales related to  $\sum_i p_T^B(i)$  the uncertainty from the variation of the renormalization and factorization scale is markedly reduced compared to the LO predictions (dashed curves in Fig. 1). Here  $\xi$  is defined via

$$\mu_R^2 = \mu_F^2 = \xi \left( \sum_i p_T^B(i) \right)^2. \quad (4)$$

The resulting  $\xi$  dependence for  $\mu_R^2 = \mu_F^2 = \xi (\sum_i k_T^B(i))^2$  is shown as the solid lines in Fig. 1. In this case, the NLO two-jet cross section is essentially independent on  $\xi$  for  $\xi < 2$ . Hence, the theoretical uncertainties due to the scale variation are very small suggesting a precise determination of  $\alpha_s(\langle k_T^B \rangle)$  for different  $\langle k_T^B \rangle$  bins, where

$$\langle k_T^B \rangle = \frac{1}{2} \left( \sum_{j=1,2} k_T^B(j) \right) \quad (5)$$

Fig. 2 shows the  $\langle k_T^B \rangle$  distribution for the NLO exclusive dijet cross section. We used the parton distribution functions set GRV [16] and

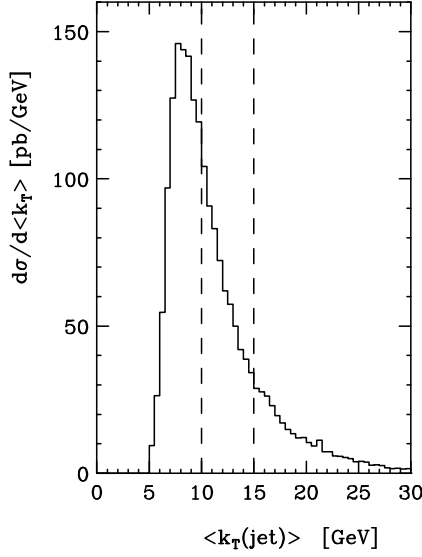


Figure 2.  $\langle k_T^B \rangle$  distribution for the two-jet exclusive cross section. The parameters are explained in the text.

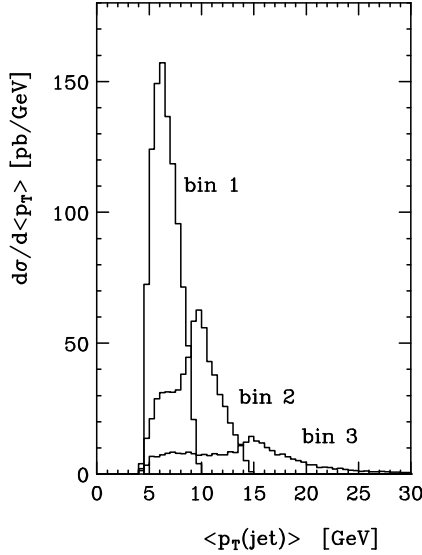


Figure 3.  $\langle p_T^B \rangle$  distribution for the three  $\langle k_T^B \rangle$  bins shown in Fig. 1.

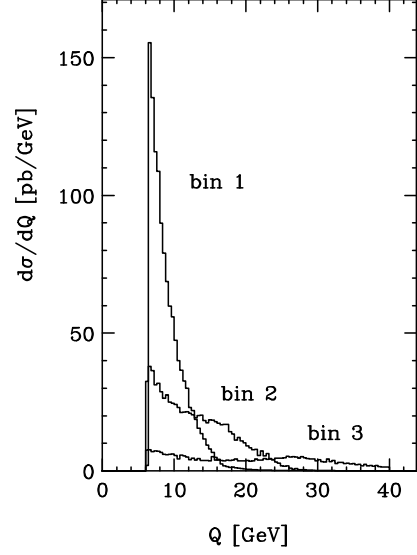


Figure 4.  $Q^2$  distribution for the three  $\langle k_T^B \rangle$  bins shown in Fig. 1.

Table 1

Jet cross sections in pb for the three  $\langle k_T^B \rangle$  bins.

	bin 1	bin 2	bin 3
GRV $\xi = 1/4$	497	320	146
GRV $\xi = 1/16$	504	306	134
GRV $\xi = 1$	488	322	151
MRSD-' $\xi = 1/4$	487	322	148

$\mu_R^2 = \mu_F^2 = 1/4 (\sum_i k_T^B(i))^2$ . In addition to the cuts imposed in Fig. 1, we require  $p_T^B > 4$  GeV for each jet and  $\sum_j k_T^B(j) > 10$  GeV. We have divided the NLO cross section in the following three  $\langle k_T^B \rangle$  bins.

bin 1:  $5 \text{ GeV} < \langle k_T^B \rangle < 10 \text{ GeV}$

bin 2:  $10 \text{ GeV} < \langle k_T^B \rangle < 15 \text{ GeV}$

bin 3:  $15 \text{ GeV} < \langle k_T^B \rangle$ .

Table 1 shows the corresponding NLO cross sections for these three bins for two different sets of parton distributions and for different values for the scale factor  $\xi$ . The theoretical uncertainties for the NLO dijet cross section from these numbers are very small, in particular for the first two bins. Fig. 3 and 4 show the  $\langle p_T^B \rangle$  and  $Q^2$  distribution for the NLO exclusive dijet cross section for these three bins. Whereas the  $\langle p_T^B \rangle$  and

$Q^2$  distributions are fairly similar to the  $\langle k_T^B \rangle$  distribution for the lowest bin, large differences are found for the other bins. This partly explains the rather different scale dependence observed in Fig.1.

### 3. Forward Jet Production in the Low $x$ Regime

Deep inelastic scattering with a measured forward jet with relatively large momentum fraction  $x_{jet}$  (in the proton direction) and  $p_T^{2lab}(j) \approx Q^2$  is expected to provide sensitive information about the BFKL dynamics at low  $x$  [ 17, 18]. In this region there is not much phase space for DGLAP evolution with transverse momentum ordering, whereas large effects are expected for BFKL evolution in  $x$ . In particular, BFKL evolution is expected to substantially enhance cross sections in the region  $x \ll x_{jet}$  [ 17, 18]. In order to extract information on the  $\ln(1/x)$  BFKL evolution, one needs to show that cross section results based on fixed order QCD with DGLAP evolution are not sufficient to describe the data. Clearly, next-to-leading order QCD corrections to the DGLAP predictions are needed to make this comparison between experiment and theory.

In Table 2 we show numerical results for the multi jet cross sections with (or without) a forward jet. The LO (NLO) results are based on the LO (NLO) parton distributions from GRV [ 16] together with the one-loop (two-loop) formula for the strong coupling constant. Kinematical cuts are imposed to closely model the H1 event selection[ 19]. More specifically, we require  $Q^2 > 8 \text{ GeV}^2$ ,  $x < 0.004$ ,  $0.1 < y < 1$ , an energy cut of  $E(e') > 11 \text{ GeV}$  on the scattered electron, and a cut on the pseudo-rapidity  $\eta = -\ln \tan(\theta/2)$  of the scattered lepton of  $-2.868 < \eta(e') < -1.735$  (corresponding to  $160^\circ < \theta(l') < 173.5^\circ$ ). Jets are defined in the cone scheme (in the laboratory frame) with  $\Delta R = 1$  and  $|\eta(j)| < 3.5$ . We require a forward jet with  $x_{jet} = p_z(j)/E_P > 0.05$ ,  $E(j) > 25 \text{ GeV}$ ,  $0.5 < p_T^2(j)/Q^2 < 4$ , and a cut on the pseudo-rapidity of  $1.735 < \eta(j) < 2.9$  (corresponding to  $6.3^\circ < \theta(j) < 20^\circ$ ). In addition all jets must have transverse momenta of at least 4 GeV in the lab frame and 2 GeV in the Breit

Table 2

Cross sections for  $n$ -jet exclusive events in DIS at HERA. See text for details.

	with forward jet	without forward jet
1 jet (LO)	0 pb	9026 pb
2 jet (LO)	19.3 pb	2219 pb
2 jet (NLO)	68 pb	2604 pb
3 jet (LO)	30.1 pb	450 pb

frame.

The cross sections of Table 2 demonstrate first of all that the requirement of a forward jet with large longitudinal momentum fraction ( $x_{jet} > 0.05$ ) and restricted transverse momentum ( $0.5 < p_T^2(j)/Q^2 < 4$ ) severely restricts the available phase space, in particular for low jet multiplicities. The 1-jet exclusive cross section vanishes at LO, due to the contradicting  $x < 0.004$  and  $x_{jet} > 0.05$  requirements. For  $x \ll x_{jet}$ , a high invariant mass hadronic system must be produced by the photon-parton collision and this condition translates into

$$\begin{aligned}
 2E(j)m_T e^{-y} &\approx \hat{s}_{\gamma,parton} \\
 &\approx Q^2 \left( \frac{x_{jet}}{x} - 1 \right) \gg Q^2, \quad (6)
 \end{aligned}$$

where  $m_T$  and  $y$  are the transverse mass and rapidity of the partonic recoil system, respectively. Thus a recoil system with substantial transverse momentum and/or invariant mass must be produced and this condition favors recoil systems composed out of at least two additional energetic partons.

As a result one finds very large fixed order perturbative QCD corrections (compare 2 jet LO and NLO results with a forward jet in Table 2). In addition, the LO ( $\mathcal{O}(\alpha_s^2)$ ) 3-jet cross section is larger than the LO ( $\mathcal{O}(\alpha_s)$ ) 2-jet cross section. Thus, the forward jet cross sections in Table 2 are dominated by the ( $\mathcal{O}(\alpha_s^2)$ ) matrix elements. The effects of BFKL evolution must be seen and isolated on top of these fixed order QCD effects. We will analyze these effects in a subsequent publication.

#### 4. Conclusions

The calculation of NLO perturbative QCD corrections has received an enormous boost with the advent of full NLO Monte Carlo programs [ 9, 20]. For dijet production at HERA the NLO Monte Carlo program MEPJET [ 2] allows to study jet cross sections for arbitrary jet algorithms. Internal jet structure, parton/hadron recombination effects, and the effects of arbitrary acceptance cuts can now be simulated at the full  $\mathcal{O}(\alpha_s^2)$  level. We found large NLO effects for some jet definition schemes (in particular the  $W$ -scheme) and cone and  $k_T$  schemes appear better suited for precision QCD tests.

The extraction of gluon distribution functions is now supported by a fully versatile NLO program. Preliminary studies show that large NLO corrections are present in the Bjorken  $x$  distribution for dijet events, while these effects are mitigated in the reconstructed Feynman  $x$  ( $x_i$ ) distribution, thus aiding the reliable extraction of  $g(x_i, \mu_F^2)$ .

For the study of BFKL evolution by considering events with a forward “Mueller”-jet very large QCD corrections are found at  $\mathcal{O}(\alpha_s^2)$ . These fixed order effects form an important background to the observation of BFKL evolution at HERA. They can now be studied systematically and for arbitrary jet algorithms.

This research was supported by the University of Wisconsin Research Committee with funds granted by the Wisconsin Alumni Research Foundation and by the U. S. Department of Energy under Grant No. DE-FG02-95ER40896. The work of E. M. was supported in part by DFG Contract Ku 502/5-1.

#### REFERENCES

1. H1 Collaboration, T. Ahmed et. al., Phys. Lett. **B346** (1995) 415; ZEUS Collaboration, M. Derrick et al., Phys. Lett. **B363** (1995) 201.
2. E. Mirkes and D. Zeppenfeld, TTP95-42, MADPH-95-916, (1995), hep-ph/9511448.
3. E. Mirkes and D. Zeppenfeld, TTP96-10, MADPH-96-935, (1996), hep-ph/9604281.
4. ZEUS Collaboration, M. Derrick et al., Z. Phys. **C65** (1995) 379; *ibid.* Phys. Lett. **B345** (1995) 576; H1 Collaboration, T. Ahmed et. al., Nucl. Phys. **B439** (1995) 471; *ibid.* Phys. Lett. **B354** (1995) 494.
5. H1 Collaboration, T. Ahmed et. al., Nucl. Phys. **B449** (1995) 3.
6. E.A. Kuraev, L.N. Lipatov and V.S. Fadin, **JETP** **45** (1972) 199; Y.Y. Balitsky and L.N. Lipatov, Sov. J. Nucl. Phys. **28** (1978) 282.
7. G. Altarelli and G. Parisi, Nucl. Phys. **126** (1977) 297; V.N. Gribov and L.N. Lipatov, Sov. J. Nucl. Phys. **15** (1972) 438 and 675; Yu. L. Dokshitzer, Sov. Phys. **JETP** **46** (1977) 641.
8. S. Catani, Y.L. Dokshitzer and B.R. Webber, Phys. Lett. **B285** (1992) 291.
9. W. T. Giele and E. W. N. Glover, Phys. Rev. D **46** (1992) 1980. W. T. Giele, E. W. N. Glover and D.A. Kosower, Nucl. Phys. **B403** (1993) 633.
10. W. Giele, these proceedings.
11. D. Kosower, these proceedings.
12. E. Laenen, these proceedings.
13. Z. Kunszt, these proceedings; S. Catani, these proceedings.
14. E. Mirkes and D. Zeppenfeld, in preparation.
15. A.D. Martin, W.J. Stirling and R.G. Roberts, Phys. Lett. **B306** (1993) 145.
16. M. Glück, E. Reya and A. Vogt, Z. Phys. **C67** (1995) 433.
17. A.H. Mueller, Nucl. Phys. **B** (Proc. Suppl.) **18C** (1990) 125; J. Phys. **G17** (1991) 1443.
18. J. Kwiecinski, A.D. Martin and P.J. Sutton, Phys. Rev. **D46** (1992) 921; J. Bartels, A. De Roeck and M. Loewe, Z. Phys. **C54** (1992) 635; W.K. Tang, Phys. Lett. **B278** (1992) 363.
19. The cuts are similar to the cuts used in the present H1 forward jet analyses. We thank A. De Roeck and E.M. Mroczko for this information.
20. H. Baer, J. Ohnemus, and J. F. Owens, Phys. Rev. **D40** (1989) 2844; Phys. Lett. **B234** (1990) 127; Phys. Rev. **D42** (1990) 61.